AEGC2019 Data to Discovery
Australasian Exploration Geoscience Conference
2-5 September 2019 • Perth, Western Australia
Incorporating the AIG, ASEG, PESA, and WABS

Ultrasonic wave velocities measurements and seismic anisotropy at Karari gold deposit: Implications for gold exploration

Andre Eduardo C. M. de Souza*
Curtin University – Expl. Geophysics
26 Dick Perry Avenue
Kensington WA 6151
a.calazans@postgrad.curtin.edu.au

Stephanie Vialle
Curtin University – Expl. Geophysics
26 Dick Perry Avenue
Kensington WA 6151
stephanie.vialle@curtin.edu.au

Andrej Bona
Curtin University – Expl. Geophysics
26 Dick Perry Avenue
Kensington WA 6151
a.bona@curtin.edu.au

SUMMARY

In order to understand the nature of reflections imaged by reflection seismic data in hard-rock environment and to investigate the seismic anisotropy across the Karari gold deposit, ultrasonic velocity measurement and seismic anisotropy studies were conducted on 18 representative samples of different alteration zones of the deposit.

The preliminary results indicate a remarkable contrast of acoustic impedance between the volcaniclastic host rock and the slightly altered zone, making this seismic interface a good guide to delimitate the mineralised zone. Furthermore, the foliated unaltered host rocks possess high values of seismic anisotropy, which must not be ignored during the seismic processing and interpretation. The anisotropy of the altered rocks is much smaller – this change in anisotropy could be potentially used as an additional parameter for seismic identification and characterisation of the altered zones.

Key words: ultrasonic wave velocity measurement, seismic anisotropy, alteration zone, Karari gold deposit.

INTRODUCTION

The major gold provinces were discovered where the ore bodies outcropped or were beneath shallow depths. However, much of gold deposits are becoming deeper or still concealed under a thick cover of unconsolidated rock and soil. Therefore, in order to have an economic impact in these areas, the exploratory activities must reduce associated drilling risks and costs. Furthermore, the accurate planning of new mines and extension of existing mines require a structural imaging in detail and a better understanding of the rock properties. In these situations, the seismic methods, with decades of successful use in the Oil & Gas industry, are an appealing geophysical tool to consider and adapt for mineral settings: they indeed join simultaneously resolution and depth of investigation. However, seismic interpretation remains largely speculative in hard-rock environments due to: (1) highly complex geologic structures, (2) scarcity of boreholes logs, (3) poor database documenting the elastic properties of rock alterations, and (4) ambiguity between strained anisotropic rock and hydrothermal alteration halos.

Direct detection of gold is extremely difficult because the ore is the minor part of the rock. However, gold deposits are commonly associated with faults and shear zones and present characteristic alteration zones when related with particular host rocks. Identifying these indirect indicators of gold mineralization could be used for targeted drilling.
Hydrothermal alteration term refers to mineralogical and textural changes of the host rocks due to the interaction with hydrothermal fluids. The alteration zone is usually used as an exploration tool to help define drill targets because it marks the pathways of hydrothermal fluids. The large-scale hydrothermal alteration system at Karari gold deposit suggests that the seismic method might be suitable for this deposit. However, petrophysical studies at laboratory or borehole should be conducted prior the seismic acquisition. Apart from few published studies (Salinbury et al., 2000; Chopping, 2008; Duff et al., 2012; Malehmir et al., 2012a; and Miah et al., 2015), the elastic properties of hard-rocks are poorly understood, therefore this topic is one of several aspects pointed by Eaton et al. (2003) and Malehmir et al. (2012b) that require further research to increase the deployment of seismic in hard rock environment.

To better understand the seismic response in hard-rock environments and to investigate the seismic anisotropy across the Karari deposit, we collected rock samples presenting different degree of hydrothermal alteration. Ultrasonic measurement of P- and S-wave velocities at atmospheric pressure and bulk density were performed.

The preliminary results show a remarkable contrast of impedance between the volcaniclastic host rock and the slightly altered zone, making this interface a good candidate for seismic delimitation of the mineralised zone. In addition, we observed high values of seismic anisotropy in the host rock due to the foliation. The results can help in interpreting existing seismic data in the area or guide future seismic acquisitions.

METHODS

Geology settings of the samples

The Karari gold deposit is situated 110 km northeast of Kalgoorlie in the east part of the Norseman-Wiluna greenstone belt of the Archaean Yilgarn Craton (Western Australia). It is part of the Carouse Dam gold camp, which also includes Whirling Dervish, Luvironza, Monty's Dam, and Twin Peaks gold deposits. Different from the typical orogenic-gold deposits of the Yilgarn Craton (Groves et al., 1998), the Karari gold deposit is an example of disseminated deposit associated with quartz-poor alkaline intrusions and presenting low gold content in quartz veins (Witt et al., 2009). In addition, the hydrothermal alteration system at Carouse Dam gold camp is extensive, several kilometres wide and at least 10 kilometres long, whereas the alteration zones associated with typical lode gold deposits in other Archean greenstone belts are more limited.

The alteration zones at Karari deposit comprise the distal propylitic (chlorite) alteration, a medial phyllic (muscovite)

zone and a potassic (biotite) alteration which grades into proximal sodic (albite) alteration adjacent to the intrusion (Gray et al., 2005; Witt and Hammond, 2008).

The gold mineralisation at Karari occurs in a fault-bound zone of volcaniclastic sedimentary rocks, which contains intrusions of monzonite porphyry and lamprophyre dykes (Gray et al., 2005; Witt et al., 2009).

Samples Description

For education purposes, Saracen Mineral Holding Limited provided a drill core to Curtin University, split into twenty-five core trays totalling approximately 100 meters of drilled rock. Lithology, alteration patterns and mineral variation of the drill core is described by Mihayo (2018) through visual inspection, X-ray fluorescence analysis, thin sections, and Scanning Electron Microscopy (SEM) analysis. Based on our own visual inspection and with the help of the analyses performed by Mihayo (2018) we selected 18 representative rock samples, covering the different stages of hydrothermal alteration (figure 1). We then classified these rock samples according to the alteration intensity of the host rock into 5 groups: unaltered fresh volcaniclastic, slightly altered volcaniclastic, moderately altered volcaniclastic, highly altered volcaniclastic and altered monzonite porphyry.

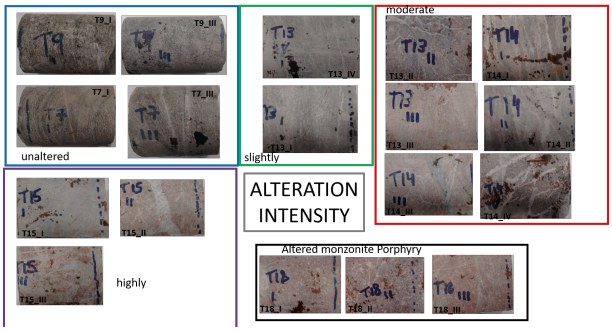

Figure 1. Photographs of the selected samples classified into 5 groups of different mineral alteration intensity.

The unaltered volcaniclastics are dominated by detrital quartz with subordinate feldspar and phyllosilicate minerals (mainly, partly deformed biotite). A well-developed foliation, defined by the preferred orientation of phyllosilicate minerals, is clearly observed on the unaltered samples. We selected four samples within this group.

Slightly altered volcaniclastic rocks show minor hydrothermal alteration in the form of potassic alteration and preserves the sedimentary structures of the unaltered volcanoclastic rock. We have two samples representing this stage of alteration. The moderately altered part of the core shows biotite-carbonate sericite alteration with pyrite dissemination are visible in the groundmass (approximately 2-3%). Some gold occurs associated with pyrite within this unit. We chose six samples that constitute the moderately altered volcaniclastic group.

At the transition between potassic and sodic alteration zones, alternating bands of relict black potassic alteration and red sodic alteration are observed (Figure 1, sample T14_I).

The highly altered volcaniclastic or sodic alteration assemblage is deep-pink to brick-red in colour and is dominated by sodic plagioclase, hosting greater amount of visible sulphides (3-5%) (Mihayo, 2018). This unit is the main mineralised zone and it is spatially influenced by monzonite porphyry intrusion. This zone is intensively cross-cut by quartz-carbonate veins and pyrite rich veinlets (Figure 1, sample T15_II and T15_III). The relict sedimentary structures are not preserved and the phyllosilicate minerals disappear at this stage of alteration. Three samples were selected to represent the highly altered volcaniclastic group and 3 to represent the altered monzonitic porphyry group.

Note that the chlorite and muscovite alteration zones were not recognized in the drill core.

Rock samples were prepared by cutting the drill cores with a rock saw into pieces 5.6 to 7.3 cm long. Care was taken to have the faces parallel for further physical properties testing. The samples from the unaltered group were cylindrical, with a diameter of 5 cm, whereas the altered samples from all groups were half cylinders.

Laboratory measurements

Bulk density and ultrasonic compressional (Vp) and shear wave (Vs) velocities measurements were carried out at Curtin Rock Physics laboratory.

For bulk density measurements, samples were oven-dried at 70°C for 24 hours. Their mass was then measured on a high-precision balance and their diameters and heights were measured with a high-precision caliper in order to compute their volumes. Bulk density was computed by dividing the mass of the sample by its volume.

Ultrasonic velocities were measured at ambient pressure and temperature conditions using the pulse transmission method (Birch, 1960), which involves measuring the travel time of the ultrasonic wave traveling through the sample. The system delay time was measured by taking head-to-head time, and then subtracted from the total travel time. We used Olympus square wave pulse/receiver (model 5077 PR) to excite the ultrasound wave in a single pair of acoustic transducers that transmits and receives P- and S-wave simultaneously, at 1 MHz of central frequency. To ensure good coupling between the samples and the transducers, we used (i) a high-viscosity bonding medium and (2) an in-house engineered device that allow applying a small, constant load on the sample surfaces. Knowing the length of the sample and the travel time of the pulse through the sample, we calculated P- and S wave velocities, Vp and Vs, respectively, by dividing the lengths by the travel times. Actual error in velocity measurement is estimated to be around 2-4% due to operator error in picking first arrival and irregular surface of some samples. The measurements were conducted along the main axis of the samples (referred to as Vp0° and Vs0°) and perpendicular to it (referred to as Vp90° and Vs90°). In the case of unaltered samples, the measurements along and transverse to the main axis coincide with the directions perpendicular and parallel to foliation, respectively.

Computation of anisotropy

A rock is considered seismically anisotropic when its velocities vary with the direction of the wave propagation. The anisotropy can be produced by preferred aligned minerals established during the deposition, known as intrinsic anisotropy; or resulting from deformation associated with applied stress, fractures, metamorphism or diagenesis, called induced anisotropy. The main symmetry system of anisotropy caused by the foliation is usually assumed as transversely isotropic (VTI).

In order to measure transverse isotropy completely and hence obtain all elastic constants (five independent stiffnesses), seismic anisotropies and Thomsen´s parameters, it is necessary to measure the velocity along three independent directions (Wang, 2002). Because of the current size and geometry limitations of our samples, and before starting a time-consuming and costly experimental procedure to get the full anisotropy tensor, we used the measured velocities in the two perpendicular directions as a first estimation of the anisotropy.

The anisotropy was quantified by two of Thomsen´s anisotropic parameters: (1) ε, which refers to the fractional difference between P velocities obtained perpendicular and parallel to symmetry axis; and (2) γ, which relates to shear anisotropy (Thomsen, 1986).

$$\varepsilon = \frac{Vp_{90°}^2 - Vp_{0°}^2}{2Vp_{0°}^2} \tag{1}$$

$$\gamma = \frac{Vs_{90°}^2 - Vs_{0°}^2}{2Vs_{0°}^2} \tag{2}$$

where V_{90} and V_0 are velocities measured perpendicular and parallel to symmetry axis.

RESULTS AND DISCUSSIONS

Table 1 summarizes the measured values of bulk densities, P- and S-waves velocities along and perpendicular to the main axis (Vp0°, Vs0°, and Vp90°, Vs90°, respectively), ε and γ Thomsen´s parameter, acoustic impedance and reflections coefficients. P-wave velocities and ε are also reported in Figure 2.

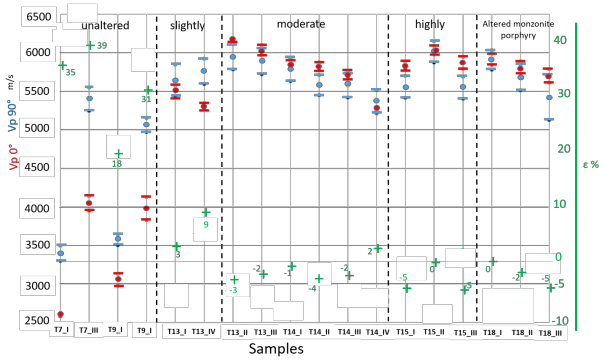

Figure 2. P-wave velocity along the main axis of the cylindrical samples (Vp0° in red), and transverse to it (Vp 90° in blue) along, and ε (green cross) for the rock samples of different mineral alteration intensity. Horizontal bars indicate maximum and minimum values obtained by repeated measurements.

For all unaltered samples, the fast wave-propagation axis is parallel to the foliation, as expected. Epsilon parameter (ε) on the rock samples of this group varies from 18% to 39% (Table 1 and Figure 2). The identification of shear wave first arrival time on unaltered samples was extremely difficult due to the overlapping of reflected P-waves and a high noise-to-signal ratio. Therefore, it was only possible to estimate γ in one sample of the unaltered rocks (T7_III), which is 37%. On the other hand, on all the altered rocks the fast shear wave signal was clear in both directions of acquisition. For almost all altered samples, in both directions of acquisition, the P- and S-wave velocities were close (Table 1 and Figure 2). Therefore, ε and γ on altered rocks are lower, 5% and 6%, respectively, except for sample T13_IV that presents visible cracks and relict foliation. The negative values of ε and γ on altered samples indicate that P- and S- velocities are faster along the main axis (Vp0° and Vs0°) than perpendicular to it (Vp90° and Vs90°), mainly because the foliation is not preserved. We expected higher values of anisotropy in samples cross-cut by visible veins (see for example samples T14_IV and T15_II in Figure 1) but these veins also appear to be randomly distributed. However, we must not forget that anisotropy is scale dependent (Mavko et al., 2009), so the overlap of aligned veins in a seismic scale must be investigated. In addition, these rocks have been offset along a series of major faults and fractures, creating a suitable environment to present seismic anisotropy in a seismic scale.

We observed a large difference in P- and S-wave velocities along the main axis (Vp0° and Vs0°) between unaltered and altered samples. On average, Vp0° is 3420 m/s, and Vs0° is 1950 m/s for unaltered samples compared to 5770 m/s and 3550 m/s on average for Vp0° and Vs0° for the altered samples. On the other hand, the difference in velocities between altered and unaltered samples is less pronounced for Vp90° and Vs90°, mainly due to higher values and bigger differences in the measured values for unaltered samples: sample T7-III exhibit a Vp90° velocity of 5400 m/s, which is close to that of sample T14-IV measured at 5370 m/s.

However, the discrimination among the groups of different intensity of alteration through the seismic velocities is difficult because there is no clear difference between them; the variation in velocities within a group (from 120m/s to nearly 500 m/s) is of the same order of magnitude as between the groups (for example, the average Vp, considering both direction of acquisition, is 5550 m/s for slightly altered, 5750 m/s for moderately altered and 5810 m/s for highly altered). Note that sample T13_IV, which exhibits the lowest velocity values, has visible cracks.

To quantify these observations, we calculated the reflection coefficients between each rock group. To obtain these reflection coefficients (displayed in Table 1), we considered normal-incidence of P-wave and used the average acoustic impedance of each alteration group (Equation 3). In addition, we assumed five layers and four interfaces with the unaltered samples at the top and the progressive increasing of the alteration towards the bottom of the drill core.

$$Rpp(0°) = \frac{I_2 - I_1}{I_1 + I_2} \tag{3}$$

with I_i the acoustic impedance of layer i and I_{i+1} the acoustic impedance of the adjacent layer. According to Salisbury et al. (2000), the estimated minimum reflection coefficient required to give a strong reflection is ±0.06. Therefore, the reflection coefficient is extremely low among the altered groups, which is not enough to be detected by the seismic method. On the other hand, the reflection coefficient between unaltered and slightly altered rocks, equal to 0.293, is sufficiently high to produce a strong, detectable reflection. Therefore, this first assessment of the seismic response gives encouraging results with regards to the use of seismic method for detection of alteration zones. However, due to the wide range of measured acoustic

impedances in the unaltered rock group, more rock samples are needed to be tested.

In contrast to sedimentary rocks, for which physical properties are controlled by porosity and by the saturating fluid, for hard-rock environment, physical properties are governed mostly by their mineralogy. In particular, pyrite (a sulphide mineral), which is dense (bulk density of 5.0 g/cm^3) and presents a P-wave velocity as high as 8000 m/s (Salisbury et al., 1996), can strongly affects the overall velocity of the mineral assemblage, depending on its content. As many worldwide gold deposits, Karari deposit has a close relationship between gold mineralisation and sulphide content because sulphidization induces gold precipitation (Groves et al., 1998). Although the quantitative mineral identification of the selected samples was not performed, Mihayo (2018) noted through visual inspection that the pyrite content increases as function of alteration within the drill core. Therefore, the high values of acoustic velocities of the altered samples, compared to the unaltered samples, may be attributed to the pyrite content. In addition, altered samples present bulk density higher than unaltered samples, probably also due to the increase of pyrite content. The difference is around 0.23 g/cm^3 in the interface between the slightly altered and unaltered samples. However, as pyrite content increases with alteration, we would have expected not only a large difference between unaltered and altered samples, but also a progressive change in velocities and densities with the degree of alteration. This suggests that other factors than pyrite content control the stiffness and a more detailed textural and mineralogical analysis of the samples is needed.

It is expected that the high values of anisotropy obtained in the unaltered rocks affect basic steps of seismic processing and interpretation. Therefore, we must further explore the results obtained in this research in order to assess their impact on seismic imaging and the ore body characterization at Karari deposit. Knowing this, we recommend more measurement of seismic anisotropy on samples across the shear zones in order to understand the relation between the deformation of the rocks and the seismic anisotropy. Doing this, we will be able to characterize and predict the seismic reflections around the structures that control the gold mineralisation. In addition, the seismic modelling must be performed over a geologically realistic representation of the Karari deposit to check the detectability of the ore body by the seismic method considering the effects of the seismic wave propagation, anisotropy, geometrical characteristics and acoustic properties of the rocks simultaneously.

CONCLUSIONS

Measurements of ultrasonic wave velocity and seismic anisotropy were conducted in the laboratory on 18 rock samples representative of different alteration zones at Karari gold deposit, Western Australia. The results of these measurements show that seismic discrimination between the different alteration zones is difficult, but a large contrast in both velocities and densities between unaltered and altered samples can be observed. A strong anisotropy is also observed in the unaltered host rock samples, in agreement with the visible foliated texture of the samples, whereas anisotropy of all altered samples is low. The large-scale alteration zone at Karari deposit favours the detectability of this geological interface by the seismic method. Any seismic processing and imaging should, however, take into account the strong seismic anisotropy in the host rocks.

ACKNOWLEDGEMENTS

We thank Saracen Mineral Holding Limited for providing the drill core. We also thank Mehrooz Aspandiar and Andrew Wieczorek, from Department of Applied Geology, for help in the selection and preparation of the samples. Andre Souza would like to thank Curtin University and CSIRO (through the Deep Earth Imaging Program) for financial support and the physical facilities for this research. He also would like to thank Professor Maxim Lebedev, from Department of Exploration Geophysics at Curtin University, for his teachings on ultrasonic velocity measurement.

REFERENCES

Birch, F., 1960. The Velocity of Compressional Waves in Rocks to 10 Kilobars, Part 1. Journal of Geophysical Research, 65, 1083-1102.

Chopping, R., 2008. Geophysical signatures of alteration. Project A3 Final Report. Predictive Mineral Discovery Cooperative Research Centre, Geoscience Australia.

Duff, D., Hurich, C., Deemer, S., 2012. Seismic properties of the Voisey's Bay massive sulphide deposit: insights into approaches to seismic imaging. Geophysics 77, WC59–WC68.

Eaton, D., B. Milkereit, and M. Salisbury, 2003. Hardrock seismic exploration: Mature technologies and adapted to new exploration targets, Foreword to hardrock seismic exploration: SEG, 1-6

Gray, D.J., Robertson, I.D.M., Cornelius, M., Sergeev, N.B., Porto, C.G., 2005. Karari and Whirling Dervish gold deposits, Western Australia. Cooperative Research Centre for Landscape Environments and Mineral Exploration (CRC LEME), CSIRO Exploration and Mining, Bentley, West. Aust.

Groves, D., Goldfarb, R. J., Gebre-Mariam, M., Hagemann, S. G. and Robert, F. 1998. Orogenic gold deposits: a proposed classification in the context of their crustal distribution, and relationship to other gold deposit types. Ore Geology Reviews 13, 7–27.

Mavko G., Mukerji T., and Dvorkin J. 2009. *Rock Physics Handbook*. Cambridge University Press. ISBN: 987-0-521-86136-6.

Malehmir, A., Andersson, M., Lebedev, M., Urosevic, M., Mikhaltsevitch, V., 2012a. Experimental estimation of velocities and anisotropy of a series of Swedish crystalline rocks and ores. Geophys. Prospect. 61, 153–167.

Malehmir, A., Durrheim, R., Bellefleur, G., Urosevic, M., Juhlin, C.,White, D.J., Milkereit, B., Campbell, G., 2012b. Seismic methods in mineral exploration and mine planning: a general overview of past and present case histories and a look into the future. Geophysics 77, W173–W190.

Miah, K., Bellefleur, G., Schetselaar, E., Potter, D. 2015. Seismic properties and effects of hydrothermal alteration on Volcanogenic Massive Sulfide (VMS) deposits at the Lalor Lake in Manitoba, Canada. Journal of Applied Geophysics 123, 141-152

Mihayo, F. 2018. Geology of the Karari deposit, Leonora, WA: Investigation of a mineralised core. Master thesis, Curtin University

Salisbury, M.H., Milkereit, B., Bleeker, W., 1996. Seismic imaging of massive sulphide deposits:part I rock properties. Econ. Geol. 91, 821–828.

Salisbury, M.H., Milkereit, B., Ascough, G., Adair, R., Matthews, L., Schmitt, D.R., Mwenifumbo, J., Eaton, D.W., Wu, J., 2000. Physical properties and seismic imaging of massive sulphides. Geophysics 65 (6), 1882–1889.

Thomsen, L., 1986, Weak elastic anisotropy: Geophysics, **51**, no. 10, 1954-1966.

Wang, Z. 2002. Seismic anisotropy in sedimentary rocks, part 2: Laboratory data." GEOPHYSICS, 67(5), 1423-1440.

Witt, W.K., Hammond, D.P., 2008. Archean Gold Mineralization In An Intrusion-Related, Geochemically Zoned District-Scale Alteration System In The Carosue Basin, Western Australia. Economic Geology 103, 445-454

Witt, W.K., Mason, D.R., Hammond, D.P., 2009. Archean Karari gold deposit, Eastern Goldfields Province, Western Australia: a monzonite-associated disseminated gold deposit. Australian Journal of Earth Sciences 56, 1061-1086.

Table 1. Summary of elastic wave velocities (in m/s), ε and γ (in%) (in%) and density (in g/cm ^{3}). V 0° = velocity parallel to the symmetry axis (perpendicular to foliation in case of unaltered rocks) and V 90° = velocity perpendicular to symmetry axis (parallel to foliation in case of unaltered rocks). For reflection coefficient, please see the text.

Samples	Alteration Intensity	Vp90°	Vp0°	ε	Vs90°	Vs0°	γ	Density	Acoustic Impedance	Reflection coefficient
T7_I	unaltered	3400	2600	35	-	1330	-	2.70	7020	
T7_III	unaltered	5400	4040	39	3400	2580	37	2.63	10625	
T9_I	unaltered	3570	3060	18	-	-	-	2.72	8323	
T9_III	unaltered	5060	3980	31	3090	-	-	2.71	10786	
T13_I	slightly	5640	5500	3	3430	3460	-1	2.94	16170	0.293
T13_IV	slightly	5760	5310	9	3450	3340	3	3.02	16036	
T_13_II	moderated	5950	6160	-3	3590	3590	0	2.83	17433	-0.003
T_13_III	moderated	5890	6040	-2	3460	3560	-3	2.99	18060	
T_14_I	moderated	5780	5840	-1	3490	3460	1	2.77	16177	
T_14_II	moderated	5580	5820	-4	3690	3560	4	2.76	16063	
T_14_III	moderated	5580	5720	-2	3510	3360	5	3.07	17560	
T_14_IV	moderated	5370	5260	2	3290	3350	-2	3.06	16096	
T_15_I	highly	5560	5840	-5	3920	4000	-2	2.96	17286	0.010
T_15_II	highly	6010	6030	0	3670	3560	3	2.85	17186	
T_15_III	highly	5550	5870	-5	3660	3910	-6	2.82	16553	
T_18_I	Monzonite Porphyry	5910	5920	0	3490	3510	-1	2.84	16813	0.002
T_18_II	Monzonite Porphyry	5680	5810	-2	3520	3580	-2	2.79	16210	
T18_III	Monzonite Porphyry	5420	5700	-5	3460	3510	-1	3.20	18240	